P2.1 WARM SEASON CORRIDORS OF PRECIPITATION IN THE CENTRAL U.S.: STATISTICS AND FORCING MECHANISMS

John D. Tuttle[1]

National Center for Atmospheric Research[2], Boulder, Colorado

1. INTRODUCTION

During the midsummer there often exists a well-defined corridor of precipitation episodes across the central U.S. For example, in a study based upon severe weather reports, Johns (1982) noted that severe weather outbreaks often occur in series over a period of several days. In a similar climatological study, Bentley and Sparks (2003) showed a tendency for derechos to occur in families with several events occurring within several days. In a radar-based climatological study, Carbone et al. (2002) found a high frequency of long-lived coherent rainfall episodes and noted a tendency for precipitation to occur in preferred latitude bands having a slow north-south oscillation over several days. The corridor location typically persists 3-7 days (in extreme cases up to 20 days) with significant variability on the inter-seasonal time scale. A corridor may experience excessive cumulative rainfall while nearby regions fall well below normal. Understanding the nature and forcing mechanisms of the corridors thus has important implications in quantitative precipitation forecasts.

In this study a U.S. national composited radar dataset and model analyzed fields are used for the 1998-2002 warm seasons to find relationships between rainfall and model kinematic and thermodynamic fields. The warm season is defined here as the months of July and August, the time of weakest synoptic scale forcing.

2. METHODOLOGY

The data used in this study are the WSI Corporation NOWrad national composite radar reflectivity and the Rapid Update Cycle (RUC) model analysis. The properties of the radar composites include an ~2 km latitude/longitude grid with 15-min temporal resolution and 16 levels of reflectivity at 5 dBZ intervals. RUC provides data with a 40-km horizontal grid spacing and is used at 3-hour intervals in this study. While there are limitations to the assimilation process, the RUC analyses provide a good representation of the atmosphere in a convenient format.

Because of the large amounts of data being used (July and August, five years for a total of 310 days), the data are analyzed and presented in reduced dimension format where data are averaged in one dimension (latitude, longitude or time) and presented in the remaining two dimensions. An example of this process and the impetus for this study are illustrated in Figure 1. The figure shows radar data in a time-latitude format for a 10-day period in July 1998. The data were first converted to rainfall rate (mm hr^{-1}) using a standard Z-R relationship and then averaged in the longitudinal direction in two different bands- one centered over the higher terrains of the Rocky Mountains (105^o-110^oW longitude) and the other over the central plains (95^o-100^oW). The daily occurrence of convection over the Rockies extending from Mexico to the Canadian border is evident in Fig. 1a, but only a small fraction is long-lived and is able to propagate into the central plains, arriving some 8-10 hours later (Fig. 1b). The preferred latitudinal corridor of convection shows a slow oscillation with time (Fig. 1b). The focus of this study then is to understand the environmental factors that lead to the corridors and why only a small fraction of the convection that develops over the Rockies is able to reach the central plains.

To investigate the corridor problem, radar data are overlaid with various fields from the RUC analyses including winds at 300, 600 and 900 hPA levels, low-level wind shear (computed between the 900 and 600 hPa levels), and computed CAPE and convergence. CAPE is computed assuming a parcel ascent from 900 hPa. The analysis is limited to the 95^o-100^oW longitude band, an area where convection often becomes highly organized, is predominantly nocturnal and the low-level jet likely plays an important role.

Figure 2 shows an example of radar rainfall overlaid on the meridional wind component at 900 hPa, near the level of maximum low-level jet (LLJ).

[1] Corresponding author address: John Tuttle, NCAR, P.O. 3000, Boulder, CO 80307-3000. email:tuttle@ucar.edu

[2] The National Center for Atmospheric Research is sponsored by the National Science Foundation.

The LLJ reaches a peak around 9:00 UTC (all times are UTC) nearly every day with the convection located near the exit region (north side) of the jet. The interest here is to construct five-year averages. Since the location of the corridor shifts north-south with time, taking an average of Fig. 2a would smear out the signal in the latitudinal direction. To eliminate this, the centroid of the radar signal is found in the time-latitude diagrams and the radar and RUC data are shifted by the appropriate amount to bring the data to 40^{o} N as shown in Fig. 2b. This allows for the averaged RUC data to be presented with respect to the radar echoes and for the generation of diurnally averaged plots.

3. RESULTS

Figures 3 and 4 show a five-year average of radar and RUC data. In the time-latitude plot (Fig. 3a), the rainfall shows a well-defined peak at 8:00 indicating that on average the rainfall is locked to the diurnal cycle. This can be seen as well in the time-longitude plot (Fig. 3d) as a streak originating near 105^{0}W and 0:00 (over the higher terrain) and propagating eastward reaching the central plains in the early morning hours. Some fraction of the precipitation in the central plains also develops locally in the early evening, perhaps in response to the LLJ. Not surprisingly the rainfall is associated with the region of maximum CAPE values and westerly/northwesterly shear (Fig. 3c). The rainfall is just to the north of the transition from northerly shear to a more westerly component. Perhaps somewhat surprising is the location of the precipitation in the exit region of the LLJ. Although It is well known that the LLJ can play an important role in the development and maintenance of convection in the central plains (Means 1952; Augustine and Caracena 1994), it is surprising to see such a strong relationship to the LLJ in a five-year averaged dataset. The LLJ advects moist unstable air into the central plains during the evening hours and results in high CAPE values to its north. The increased convergence (divergence) to the north (south) of the LLJ (Fig. 5) can play a role in triggering (suppressing) convection locally during the evening as well. The longitude-latitude plots (Fig. 4) represent a five-year average using data between 3:00 and 12:00, the time period of maximum LLJ. The relationship between the convection and LLJ, CAPE and shear is again clearly seen in Figs. 4b,c and f. At the upper levels the flow is dominated by an anticyclone centered over Texas. The convection is situated at the top of the anticyclone in the region of strong gradients of the westerly flow. Again, note that the exit region of the LLJ is a region of strong moisture convergence and higher CAPE values. The northerly shear to the south of the convection is due to the strong southerly winds of the LLJ at the low levels and weak winds at 600 hPa.

Since the LLJ jet appears to play an important role in the location and diurnal cycle of the convection, the summary plots of Figs. 3 and 4 are produced for days which had weak (< 5 m s^{-1}) or non-existent LLJ (Figs. 6 and 7). A total of 32 days were found meeting the criteria. Convection for those days is virtually non-existent (Figs. 6a,d and 7a) and there is little evidence of convection propagating across the central U.S. CAPE values are also much lower than in the five-year average. The upper level flow is northwesterly (Fig. 7e) with the anticyclone situated well to the west over Utah and Arizona. In this dry northwesterly flow regime it is not surprising that convection and the formation of the LLJ was suppressed.

Summary plots for days which had strong LLJ (> 10 m s^{-1}, 86 days) are shown in Figs. 8 and 9. The total rainfall is somewhat larger compared to the average and while the propagation component is still evident (Fig. 8d), a greater percentage of the precipitation develops locally. This is likely the result of the increased moisture convergence associated with a stronger LLJ and parcels being able to overcome the nocturnal inversion to reach the level of free convection. CAPE values are also larger. At the upper levels (Fig. 9e) the anticyclone is stronger and is situated in eastern Texas.

The strength of the low-level wind shear is also known to be a factor in sustaining convection. Summary plots for days with weak shear (<10 m s^{-1},34 days) and moderate shear (>15 m s^{-1},19 days) are shown in Figs. 10,11 and Figs. 12,13, respectively. In the low shear cases there is a complete lack of any long-lived propagating convection (Fig. 10d) and the convection that does form occurs at the time of maximum solar heating, i.e., between 22:00 and 2:00 as opposed to 8:00 in the five year average. The LLJ is still present, but considerably weaker and CAPE values are only slightly less. At the upper levels the Texas anticyclone is much weaker with weak westerly/northwesterly flow in the convective region. Thus while the CAPE values are only slightly reduced, the precipitation pattern changes dramatically and only short-lived convection develops in response to solar heating.

In the stronger shear cases the precipitation once again is long-lived and has a strong propagation signal, with the peak rainfall occurring in the early morning hours. The LLJ has increased and the CAPE values increase slightly. The Texas anticyclone is strong and is shifted somewhat to the west. A comparison of the two sets of figures clearly demonstrate the importance of shear in maintaining convection.

4. DISCUSSION

Convection propagating across the central U.S. is often confined to a relatively narrow latitudinal corridor. Understanding why the corridor is where it is has important implications for QPF since the corridor region may experience excessive rainfall, while nearby areas may be below normal. Combining radar with RUC model analyses, plots showing five-year averages for the months of July and August were presented. While the corridor of convection showed the expected association with the area of enhanced CAPE and northwesterly/westerly shear, a somewhat surprising result was the strong correlation to the exit region of the LLJ. The LLJ plays an important role by advecting moist, unstable air into the central plains and the increased convergence aids in sustaining convection propagating into the region and in the forcing of convection locally. The nocturnal maximum in convection in the central plains is a combination of convection propagating into the region from the eastern slopes of the Rockies and that forced locally by the LLJ. As the strength of the LLJ increases, a greater percentage of the convection is forced locally. The results also showed a strong sensitivity to the strength of the low-level wind shear. For days which had low shear (<10 m s^{-1}) long-lived propagating convection was non-existent and the convection that developed was locally forced near the time of solar heating maximum and was short-lived.

In the warm season under conditions of weak synoptic conditions, the corridor of convection is strongly tied to the exit region of the LLJ. The lack of propagating convection south of the corridor is for several reasons. The low-level flow south of the LLJ is strongly divergent and the region is under-subsidence, hence convection is suppressed. Secondly the shear vector is northerly and not conducive for eastward propagating convection. Finally the steering flow at the mid-levels is weak making it difficult for convection to advect eastward. North of the corridor, the air tends to be cooler and dryer (less CAPE) and is generally less favorable for the development and maintenance of convection. Thus on average there is a relatively narrow corridor favorable for the development of long-lived propagating convection.

5. REFERENCES

Augustine, J.A. and F. Caracena, 1994 :Lower tropospheric precursors to nocturnal MCS development over the central United States. Wea. Forecasting**, 9**, 116-135.

Bentley, M.L. and J.A. Sparks. 2003. A 15 yr. climatology of derecho-producing mesoscale convective systems over the central and eastern United States. *Climate Research*, **24**, 129-139.

Carbone, R.E., J.D. Tuttle, D.A. Ahijevych, and S.B. Trier, 2002. Inferences of predictability associated with warm season precipitation episode. *J. Atmos. Sci*., **59**, 2033-2056.

Johns, R.H., 1982: A synoptic climatology of northwest flow severe weather outbreaks. Part I: Nature and significance. *Mon. Wea. Rev.*,**110**, 1653-1663.

Means, L.L., 1952: On thunderstorm forecasting in the central United States. *Mon. Wea. Rev.*,**80**, 165-189.

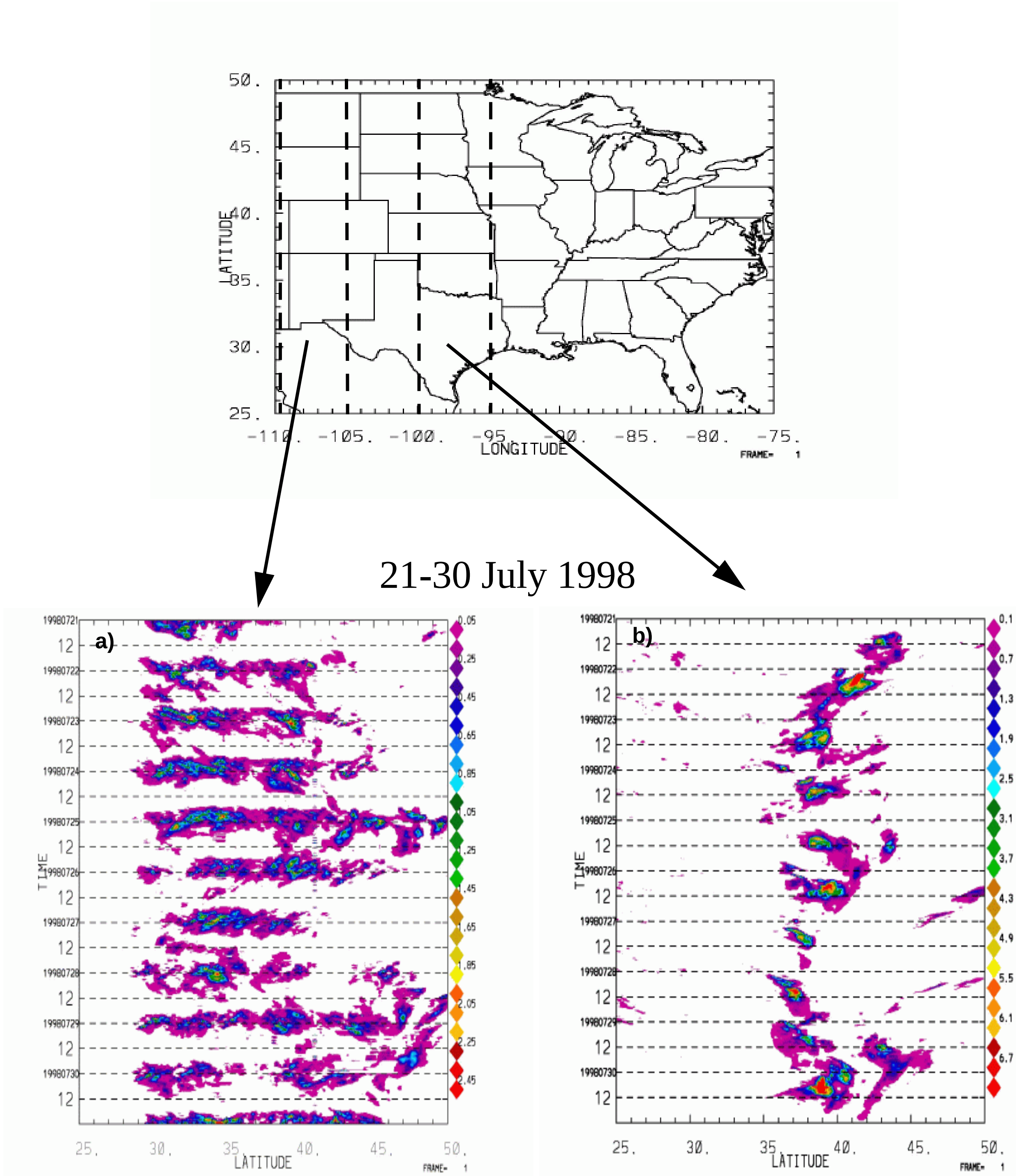

Figure 1. Time-latitude (Hovmoller) plots of radar derived rainfall rate averaged over a) 110-105^{o}W and b) 95-100^{o}W longitude bands for 21-30 July 1998.

20-30 July 1998

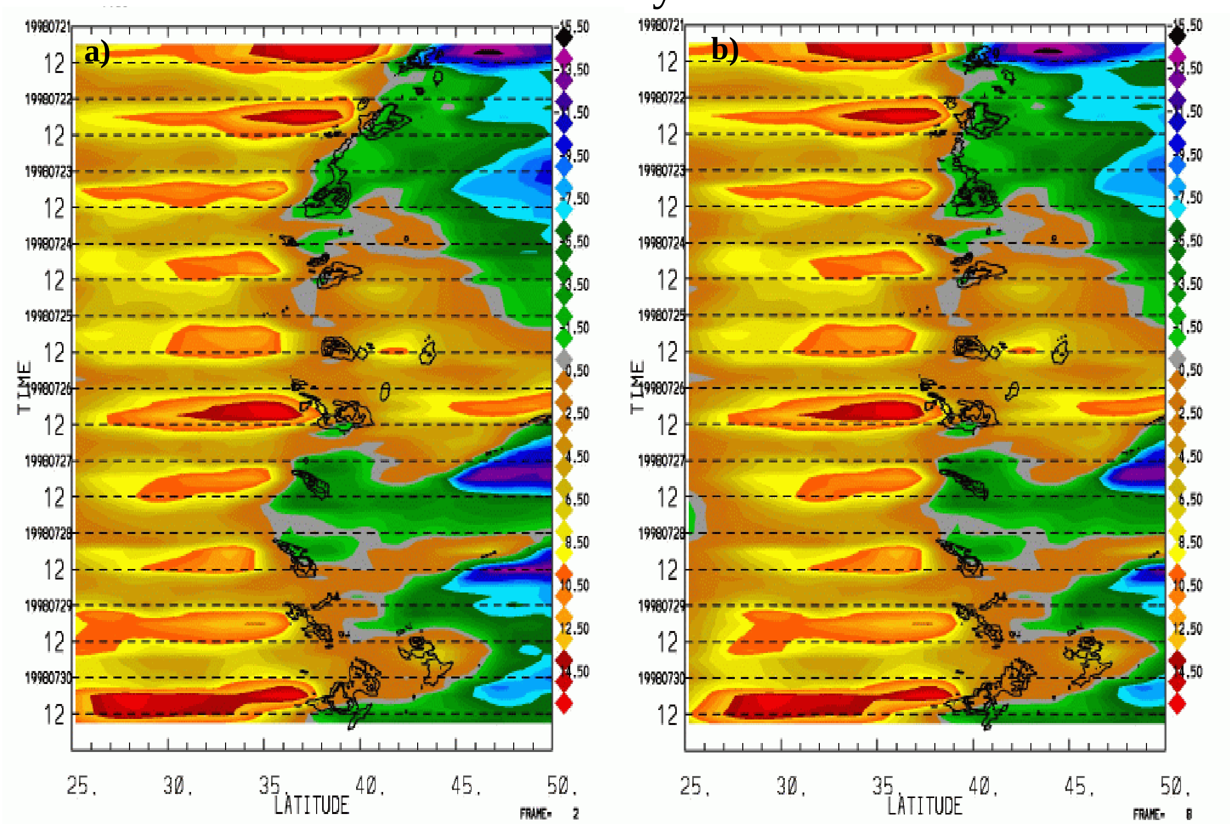

Figure 2. Time-latitude plots of radar rainfall rate (contours) superimposed on 900 hPa meridional wind for a) unshifted data and b) data shifted to 40^{o}N using the centroid of the radar data as a reference.

July-August 1998-2002

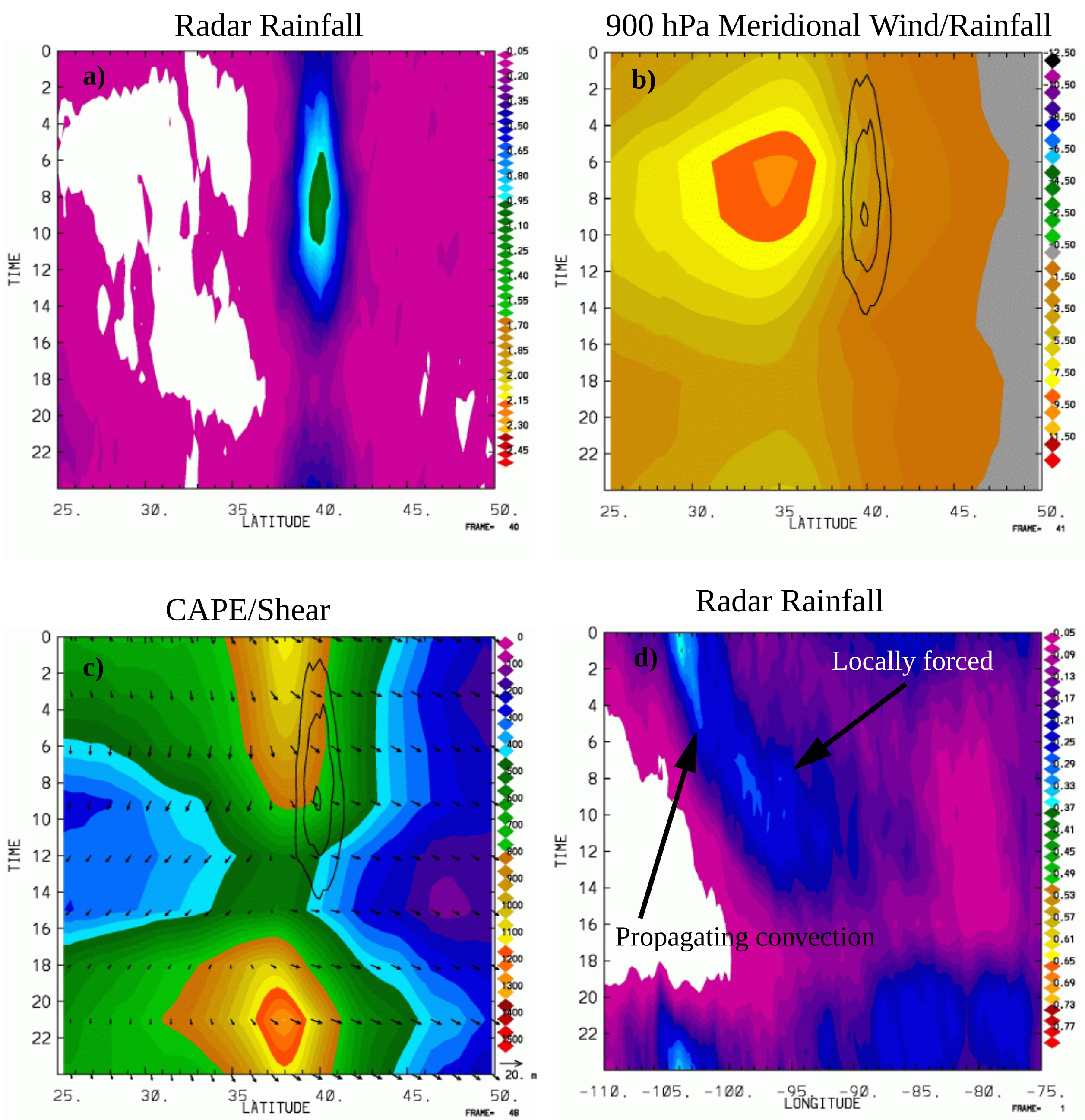

Figure 3. Diurnally averaged a) radar rainfall b) 900 hPa meridional wind and radar rainfall (contours) c) CAPE, shear (between 600 and 900 hPa) and radar rainfall (contours) in time-latitude format over the longitude band shown in Fig. 1b and d)radar rainfall in time-longitude format. For the shear vectors in c) north is taken as directed toward the top of the page in the usual sense.

July-August 1998-2002

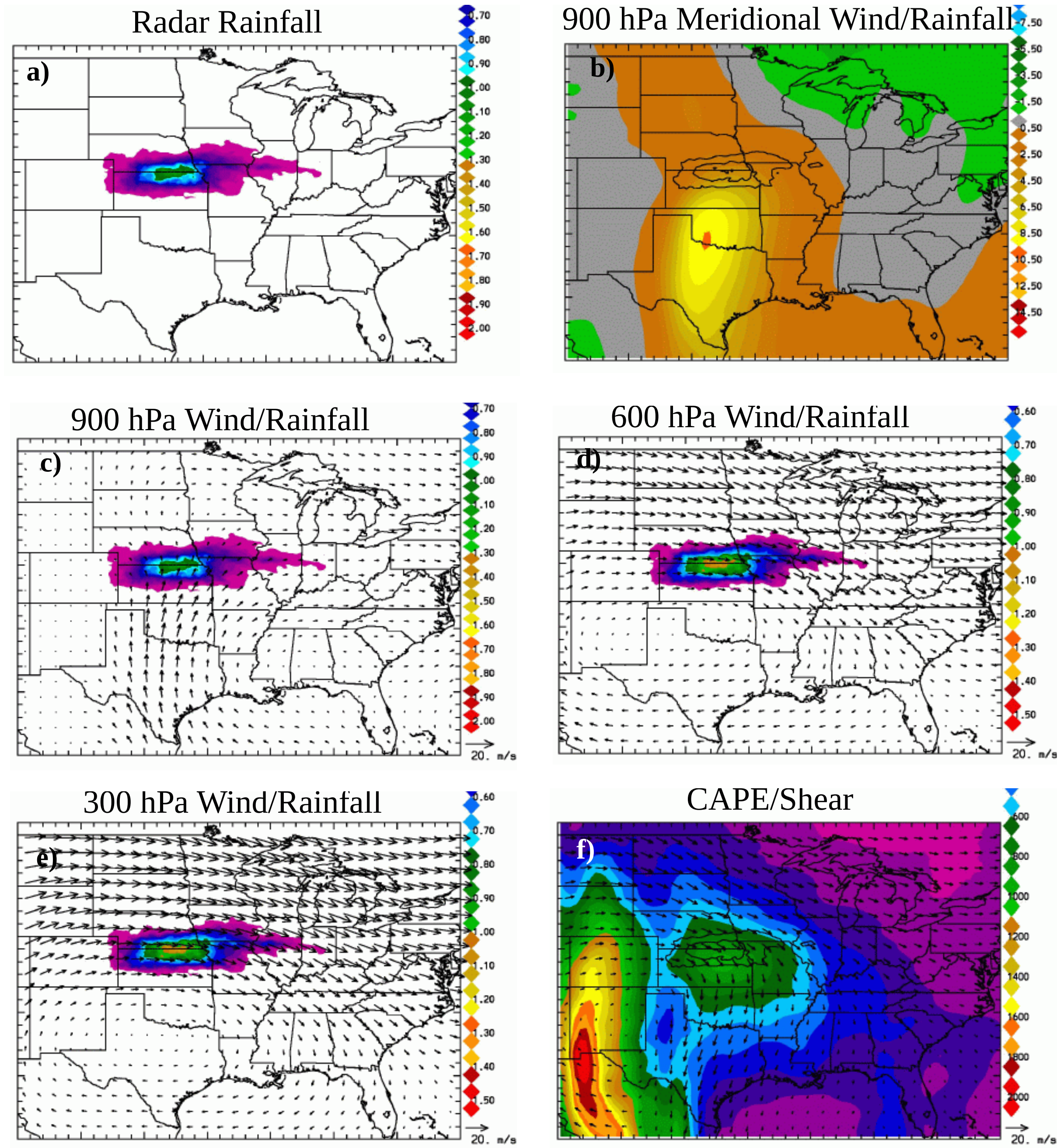

Figure 4. Averaged (310 days for times between 3:00 and 12:00) longitude-latitude plots of a) radar derived rainfall rates, b) 900 hPa meridional wind/radar rainfall (contours), c) 900 hPa winds/radar rainfall, d) 600 hPa winds/radar rainfall, e) 300 hPa winds/radar rainfall and f) CAPE/shear/ radar rainfall for July-August 1998-2002.

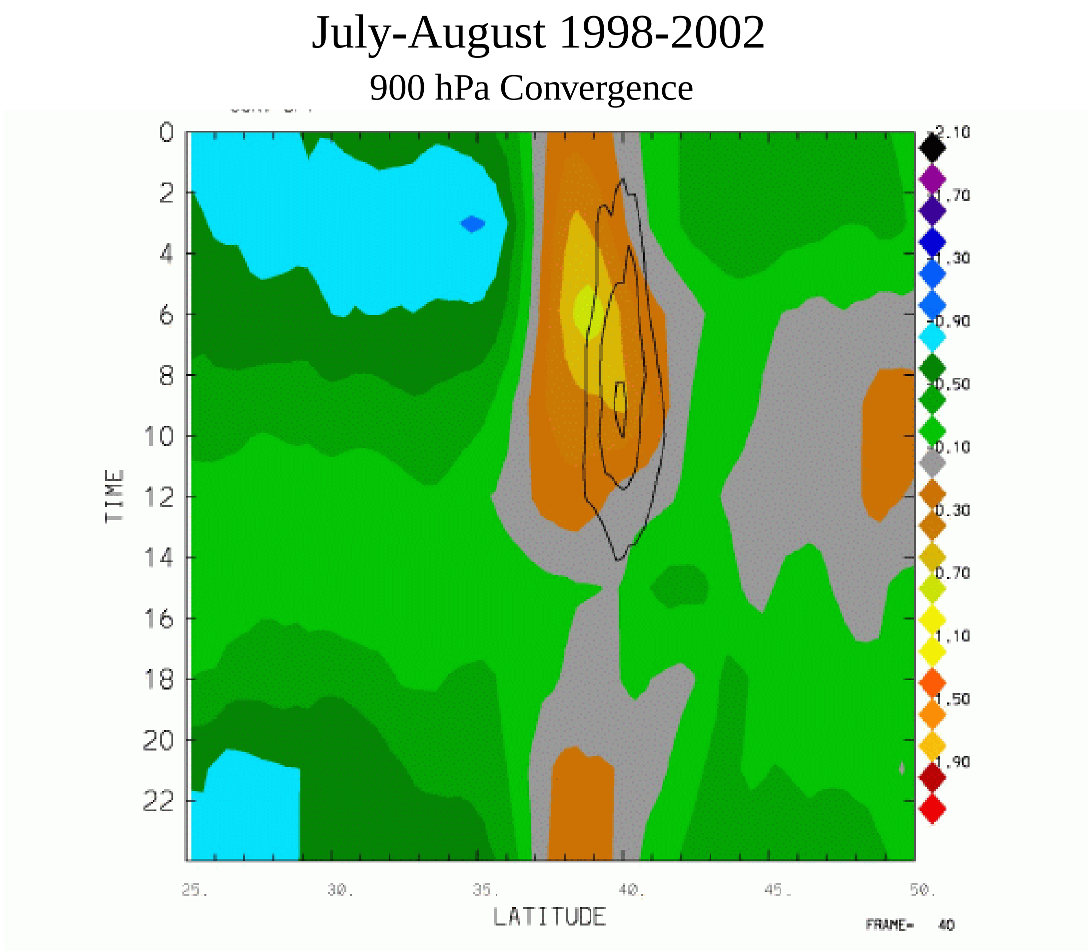

Figure. 5 Diurnally averaged 900 hPa convergence (10^{-5} s^{-1}) and radar rainfall (contours) .

July-August 1998-2002 32 days

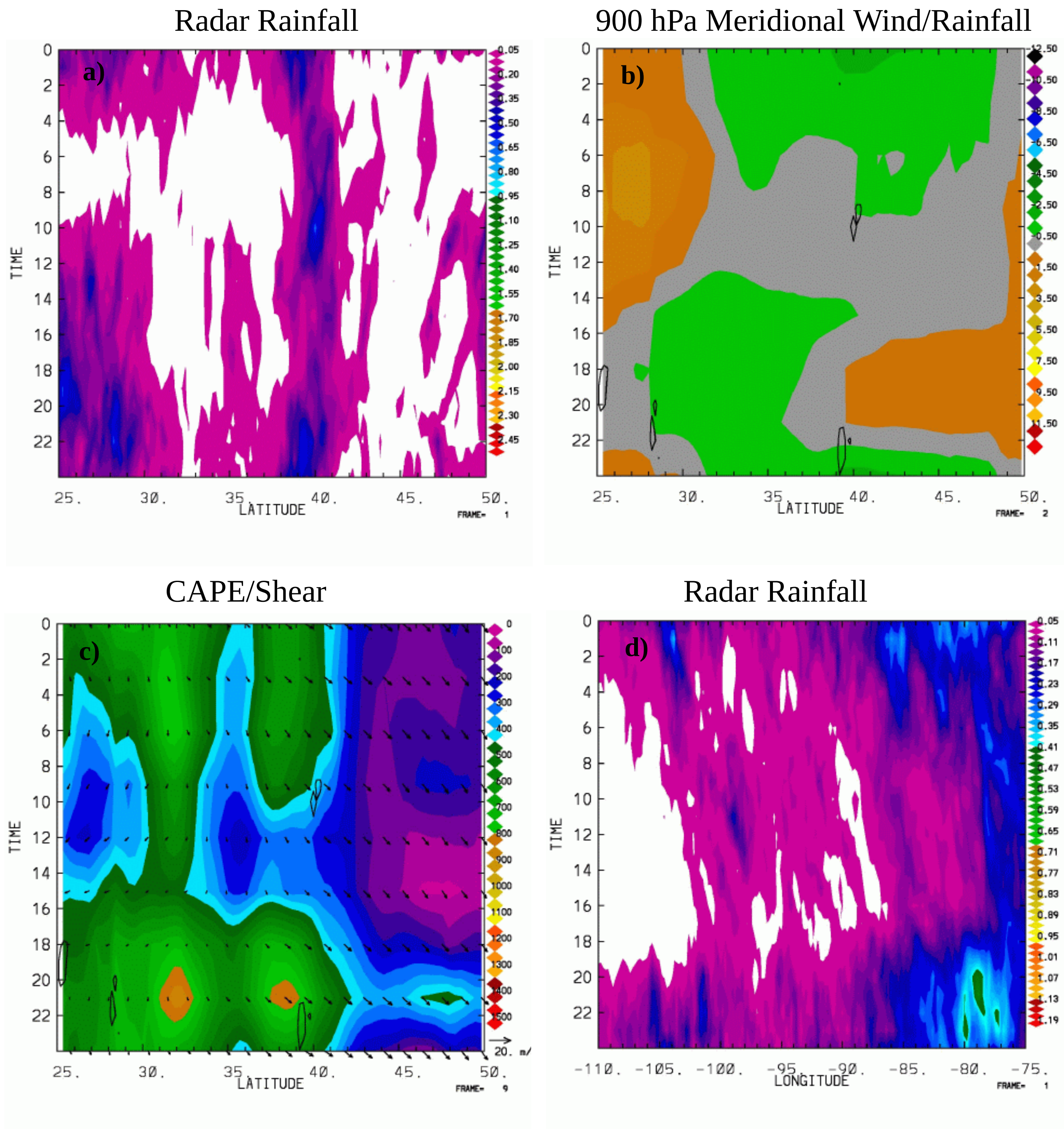

Figure 6. Same as Figure 3 except for days with LLJ < 5 m s^{-1}.

July-August 1998-2002 32 Days

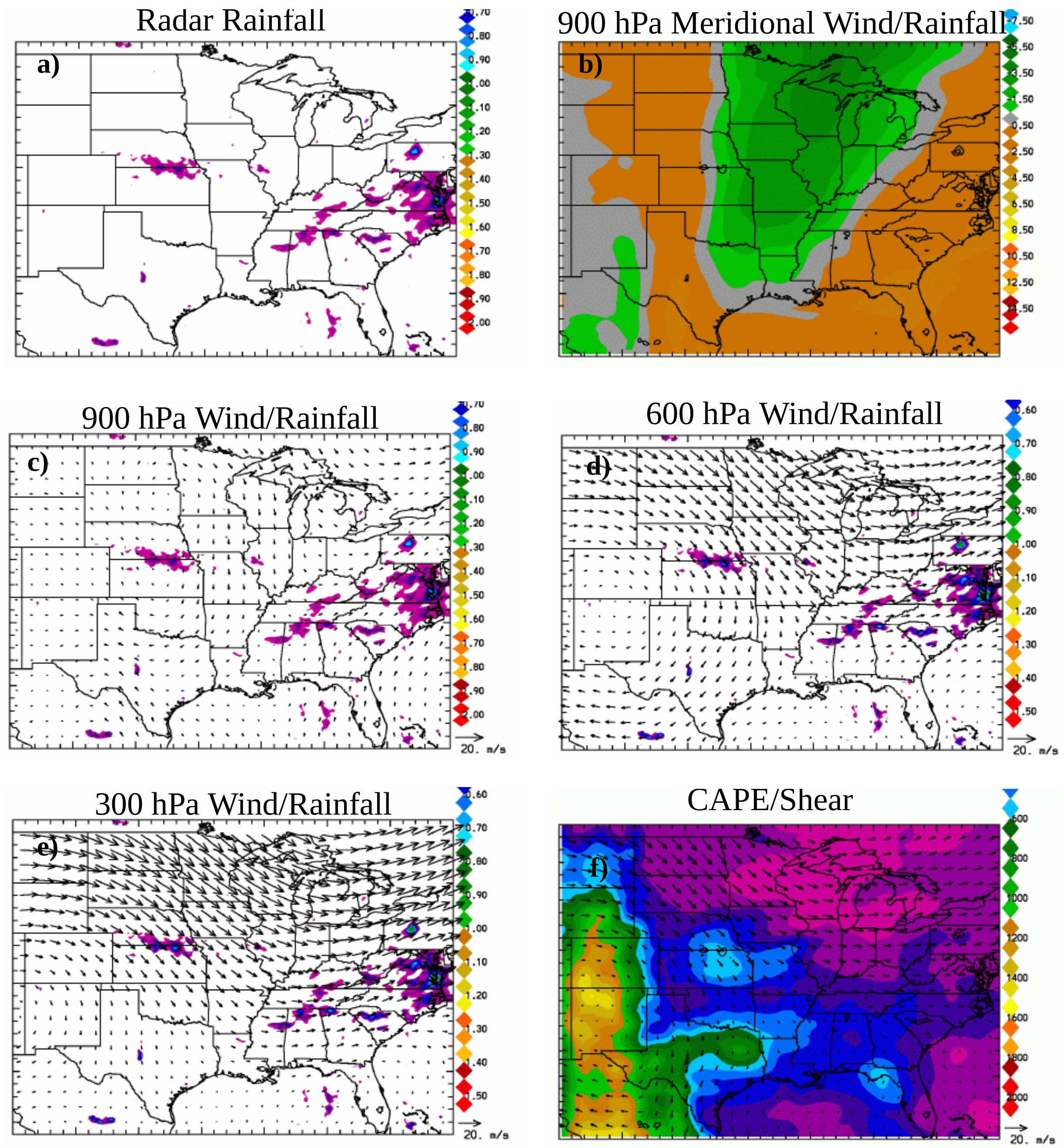

Figure 7. Same as Figure 4 except for days with LLJ < 5 m s^{-1}.

July-August 1998-2002 86 Days

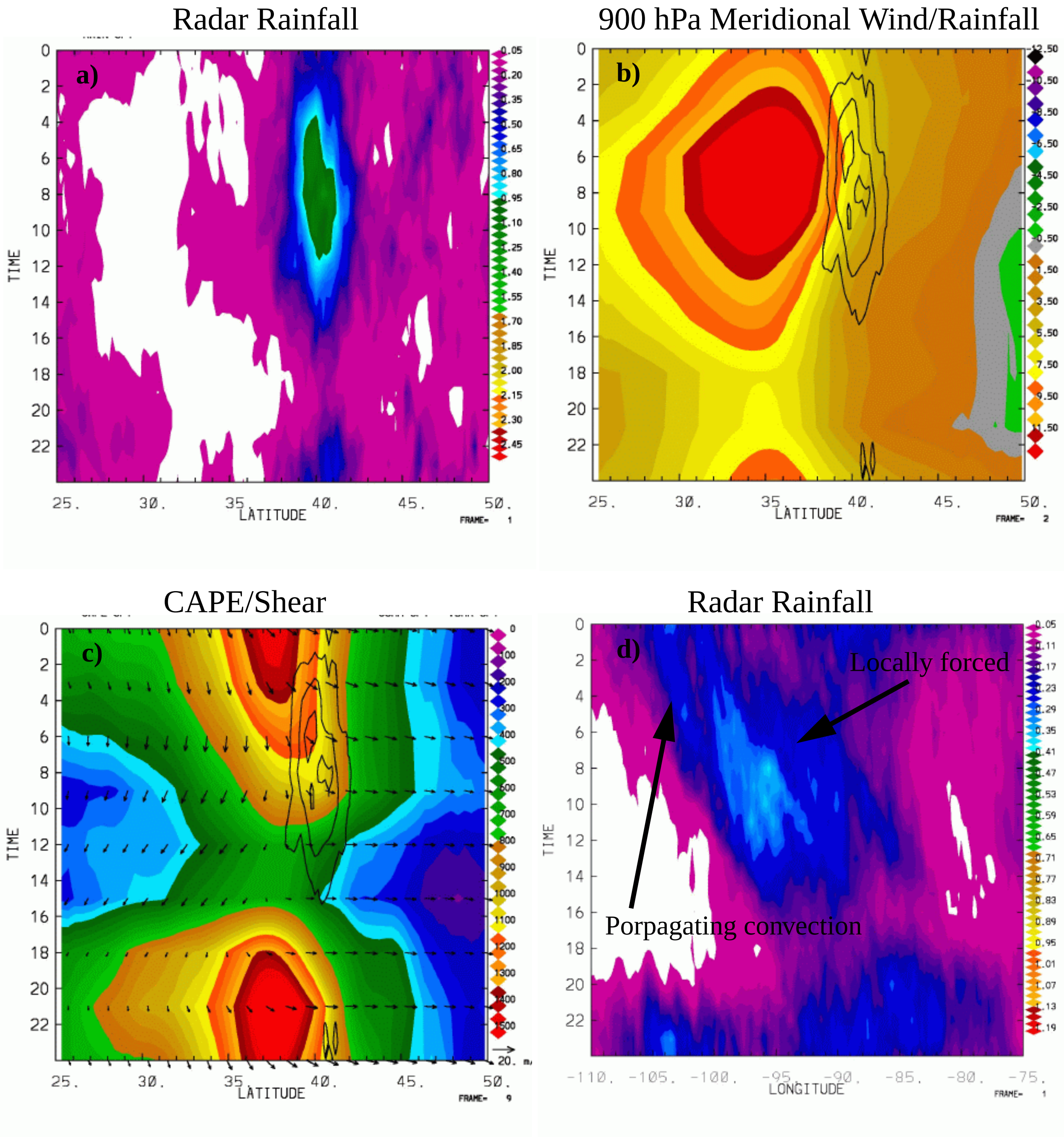

Figure 8. Same as Figure 3 except for days with LLJ > 10 m s^{-1}.

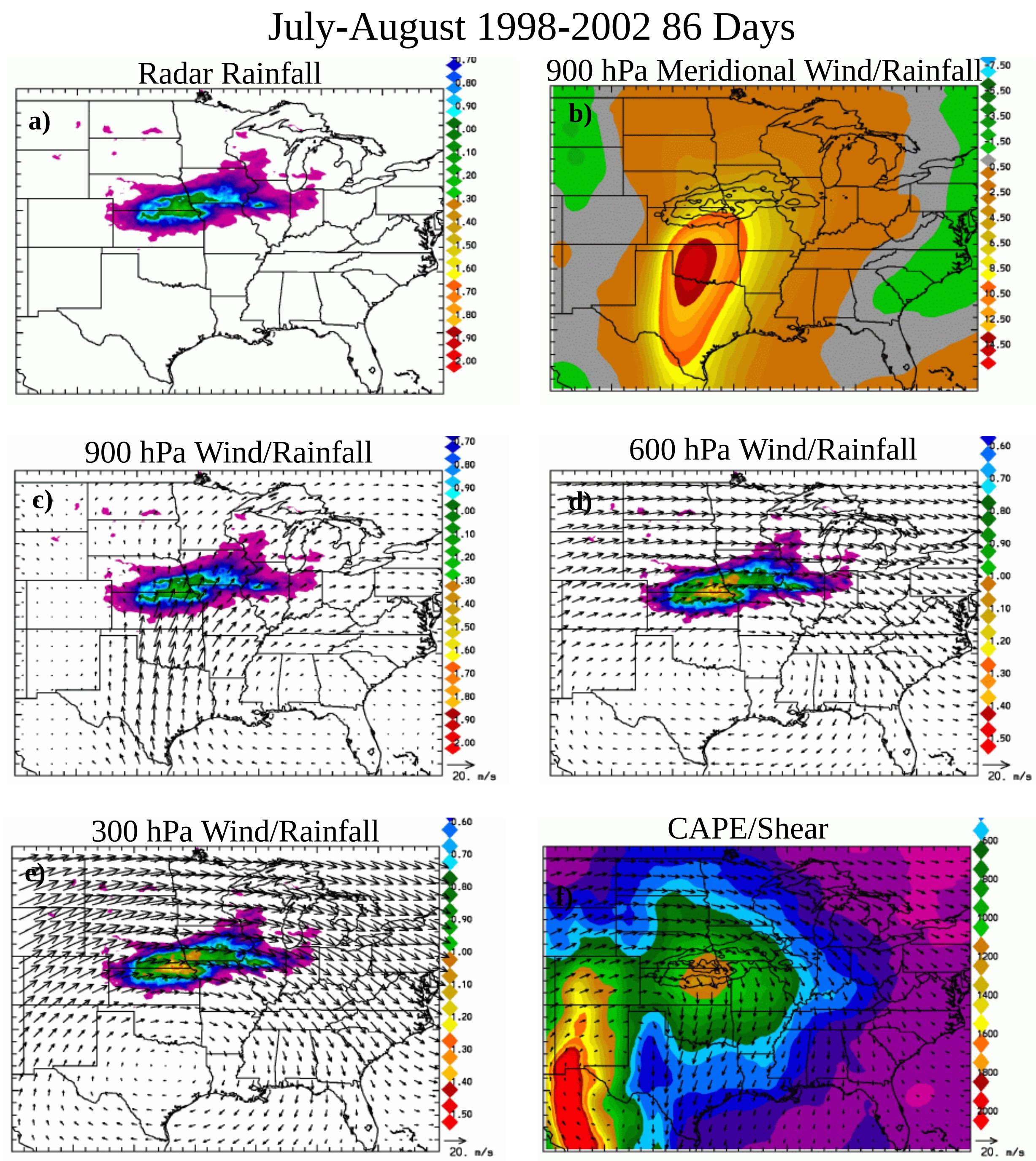

Figure 9. Same as Figure 4 except for days with LLJ > 10 m s^{-1}.

July-August 1998-2002 34 Days

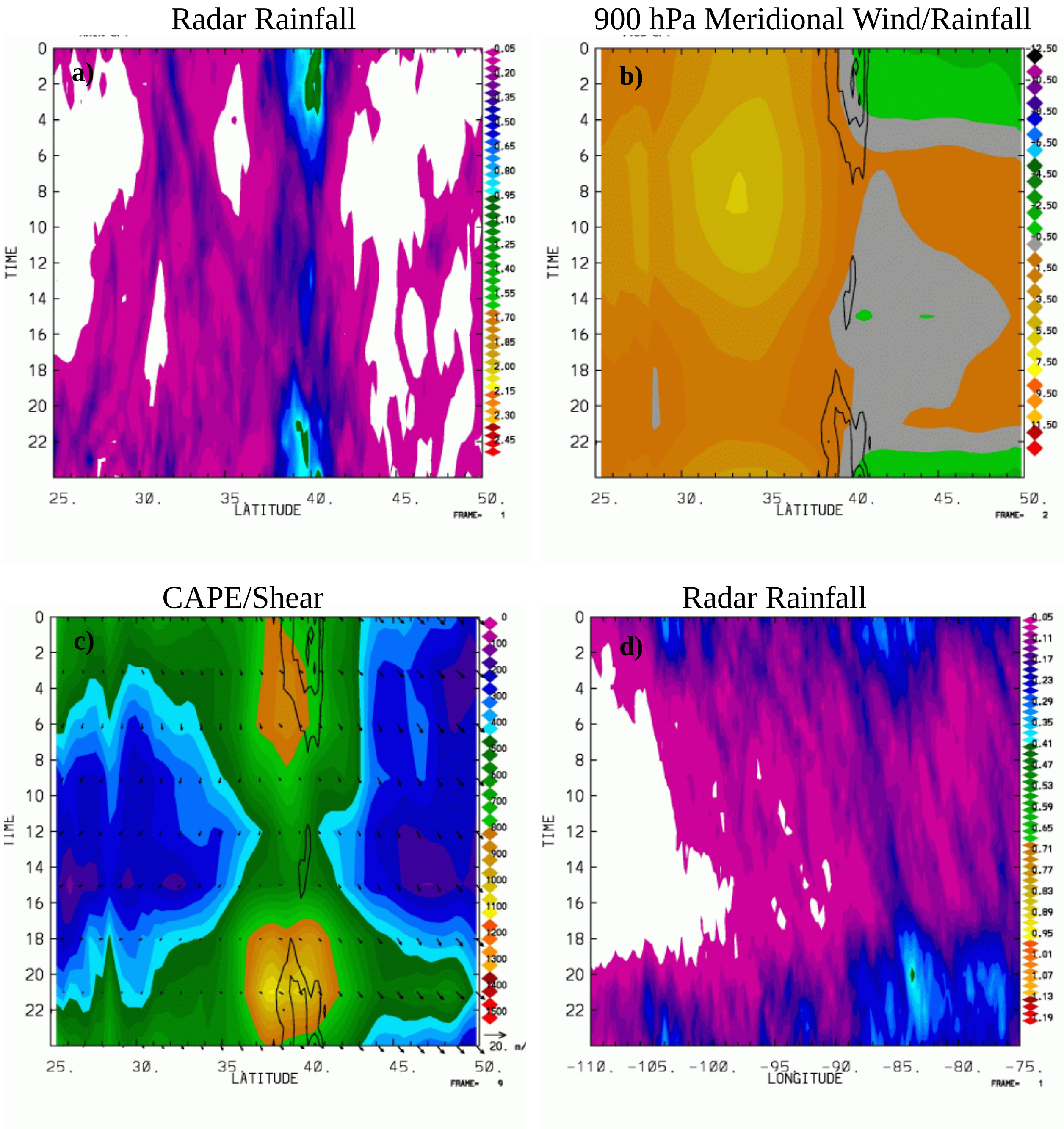

Figure 10. Same as Figure 3 except for days with low-level shear < 10 m s^{-1}.

July-August 1998-2002 34 Days

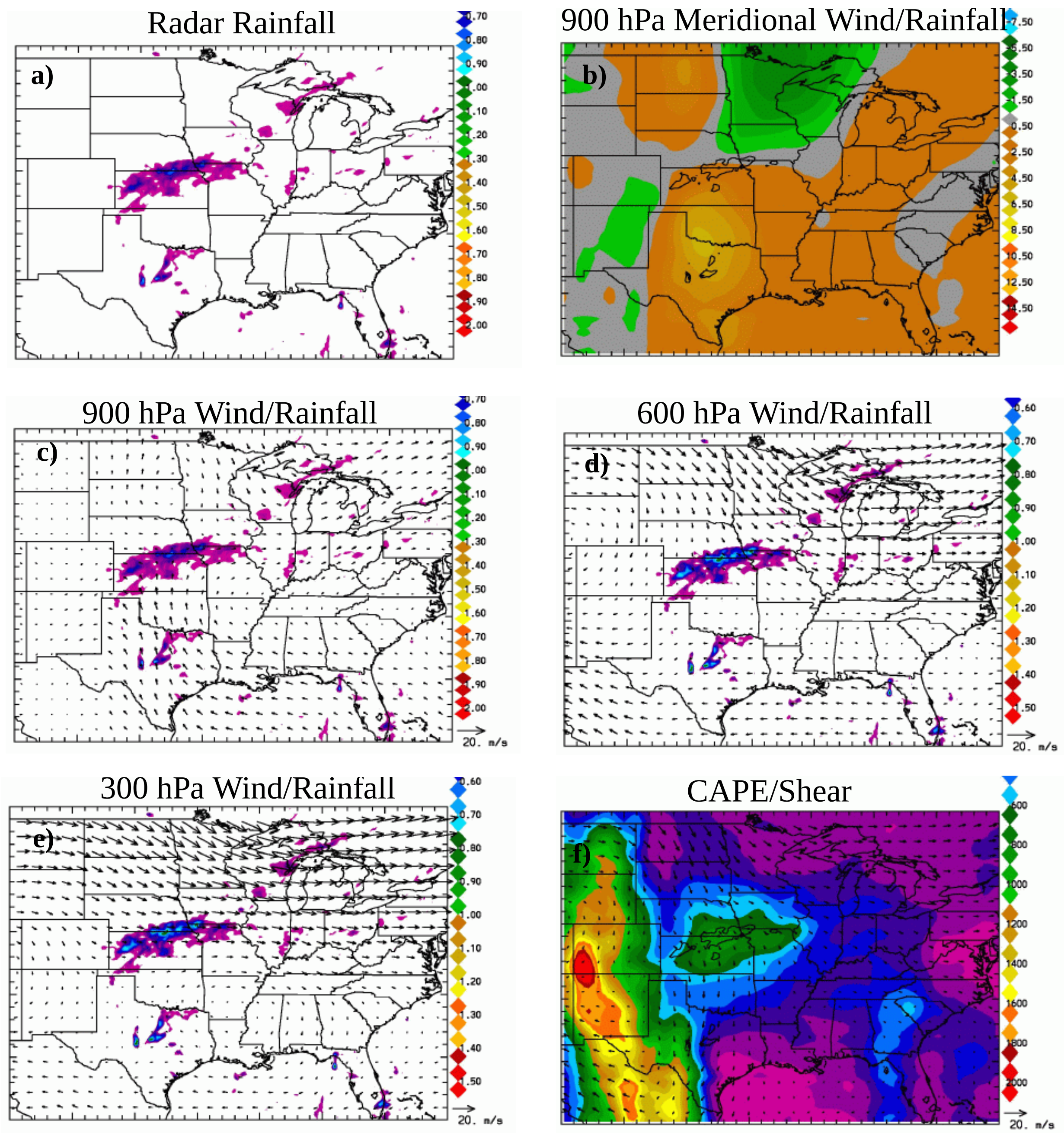

Figure 11. Same as Figure 4 except for days with low-level shear < 10 m s^{-1}.

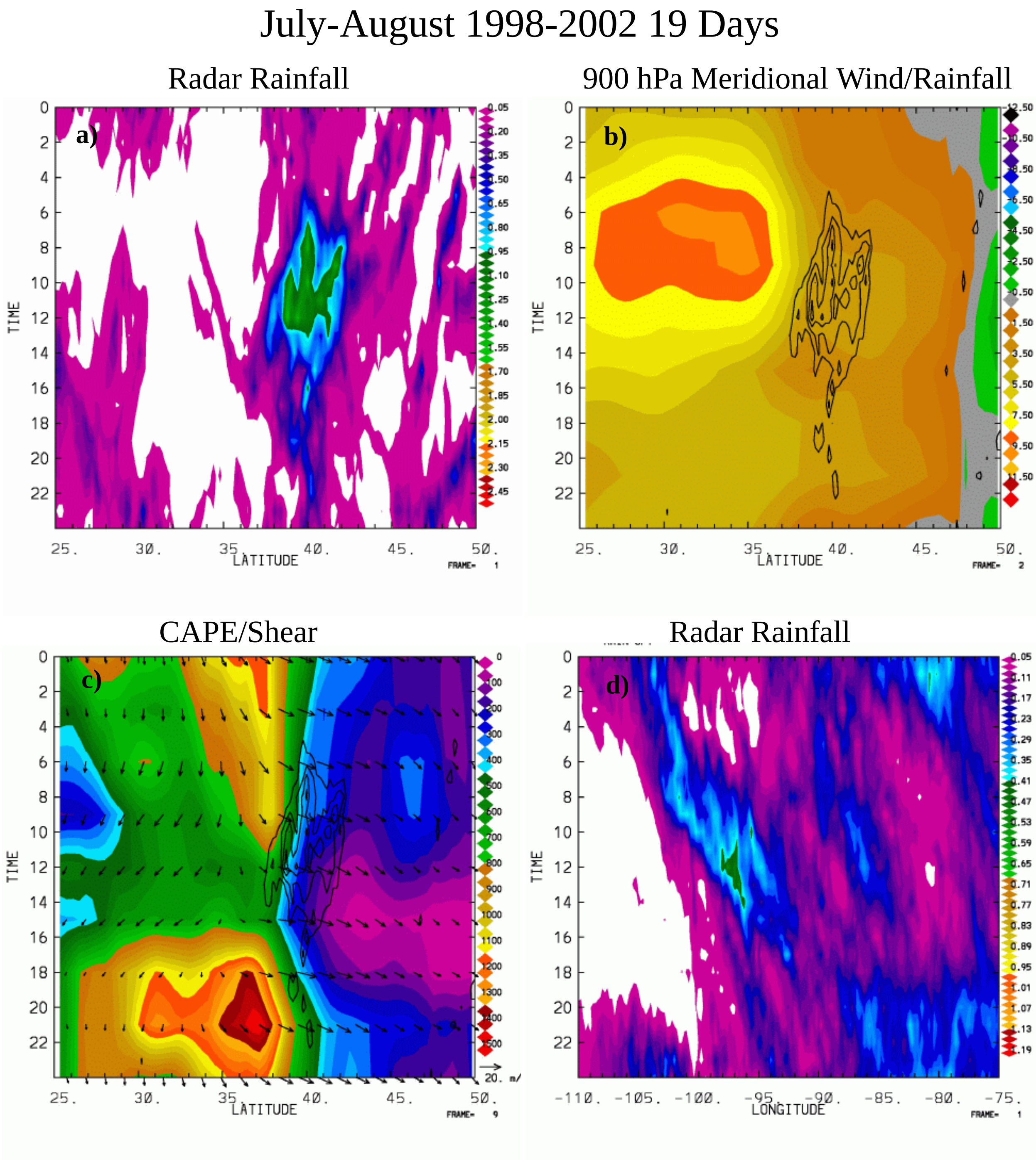

Figure 12. Same as Figure 3 except for days with low-level shear > 15 m s^{-1}.

July-August 1998-2002 19 Days

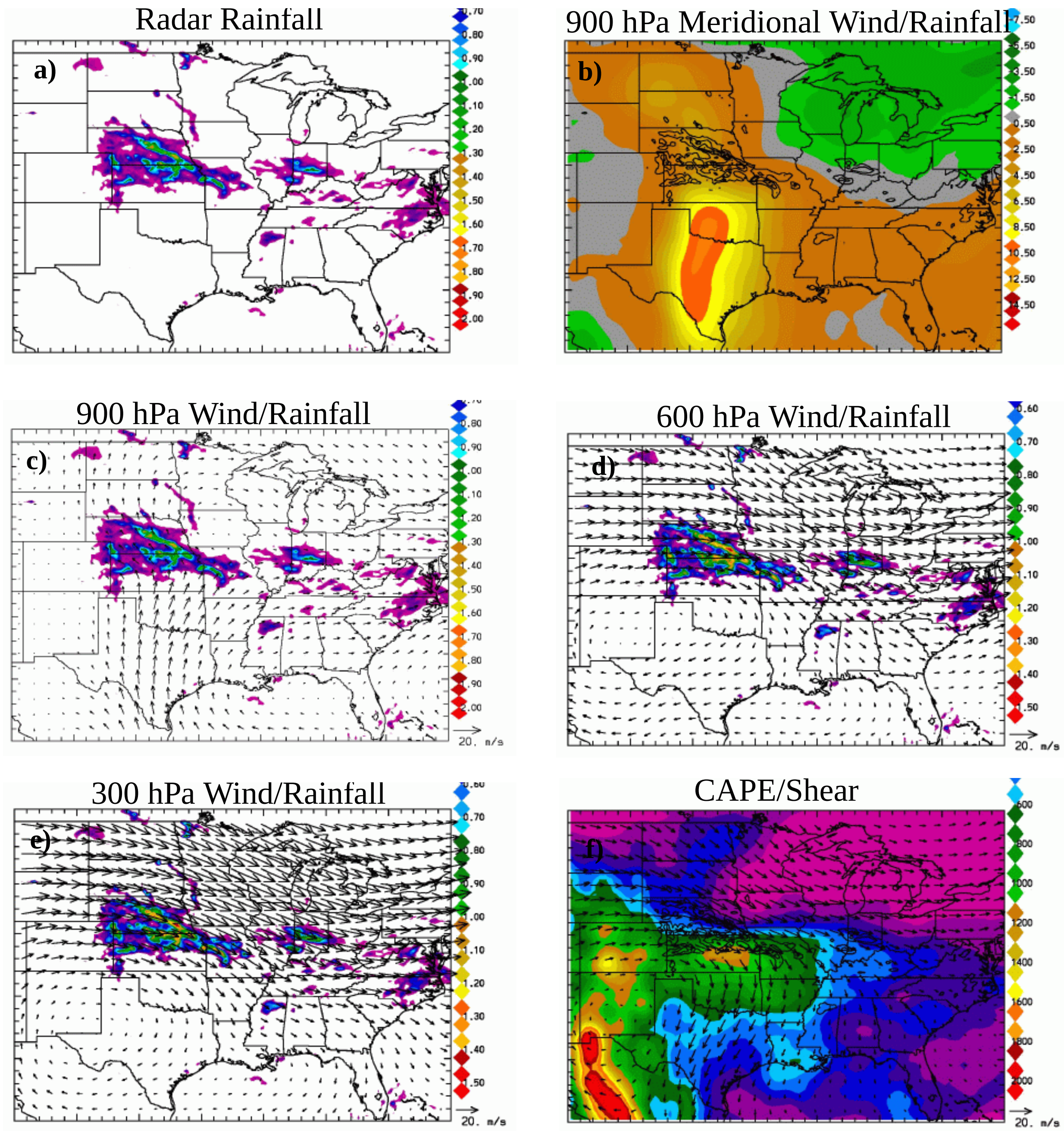

Figure 13. Same as Figure 4 except for days with low-level shear > 15 m s^{-1}.